

Role of Diffusion Tensor Imaging in Characterization and Preoperative Planning of Brain Neoplasms

Mohsen Gomaa and Yosra abdel zaher

Department of Radiodiagnosis, Ain Shams University
mostafa_redio@yahoo.com

Abstract: Background and purpose: DTI is an MR imaging measure of brain tissue integrity. It gives precise information about the involvement and integrity of the white matter tracts in the immediate region surrounding tumors. The purpose of our study is to evaluate the role of DTI in characterization and preoperative assessment of brain neoplasm. Materials and methods: 32 patients with intracranial neoplasm were included in this study which was conducted during a 2 years period. Conventional MRI before and after IV Gadolinium administration was done followed by DTI and diffusion tensor tractography, with FA and ADC values measurements of different white matter tracts in direct relation to the tumor. The values obtained were compared to the normal unaffected tract in the contralateral side. Results: White matter involvement by a tumor was classified according to the criteria of displacement, infiltration, disruption or edema. Patients were classified into two main groups according to the tumor type: Benign and Malignant groups. Prevalence of tract displacement was higher among benign group in comparison to malignant group with significant difference in between by using chi-square test (P value<0.05). While prevalence of disruption was higher among malignant group, in comparison to benign group with significant difference in between by using chi-square test. (P value<0.05). Conclusion: The information provided by DT imaging further defined precise relationships between the sub cortical white matter structures and the cerebral neoplasm. This potentially has a role in tumor characterization, and more importantly in surgical planning.

[Mohsen Gomaa and Yosra abdel zaher **Role of Diffusion Tensor Imaging in Characterization and Preoperative Planning of Brain Neoplasms**. Life Science Journal, 2012; 9(1):163-176] (ISSN: 1097-8135).
<http://www.lifesciencesite.com>

Key words: diffusion tensor imaging. Brain tumor. Preoperative planning. Glioma.

Abbreviations:

ADC: apparent diffusion coefficient **FA:** fractional anisotropy **DTI:** diffusion tensor imaging.

1. Introduction:

Before proper planning of brain surgery, it is very important to avoid several key functional regions of the brain; these include motor, sensory, auditory, language, and vision fields. We have a fair amount of knowledge about functional maps of the cortex, but we do not have equivalent maps of the white matter. The location and functions of the cortex can be deduced from the folding patterns of the cortex but the white matter appears as just a homogenous structure during surgery. Even if we avoid injury to an important cortical area, the patient could lose function if the white matter tract responsible for the function is cut. Therefore, the identification of motor, language, auditory, and visual pathways is very important for brain surgery (*Mori, 2007*).

Magnetic resonance (MR) imaging and MR Spectroscopy plays an important role in the detection and evaluation of brain tumors. In the past few years, however, a number of advanced MR imaging techniques have been developed that provide new methods for the assessment of brain tumors. One of these techniques is diffusion tensor imaging. (*Provenzale et al., 2006*).

DTI is a quantitative MR imaging technique that measures the 3D diffusion of water molecules within tissue through the application of multiple diffusion gradients (*Basser & Pierpaoli, 1996*). The power of diffusion techniques comes from measurement of molecular probing of tissue structures by water molecules at a microscopic scale well beyond the typical MR imaging resolution. By measuring the interaction of water molecules with cell membranes, myelin sheaths, and macromolecules, tissue integrity can be inferred (*Pierpaoli & Basser, 1996*). Tissue has physical structures that limit diffusion in different directions, so diffusion is typically described as a 3D ellipsoid through a 3×3 matrix. In nervous tissue, the largest (or primary) ellipsoid eigenvector represents diffusion along the length of a fiber tract and so is referred to as the $\lambda_{//}$. The other shorter 2 ellipsoid eigenvectors, when averaged together, are called λ_{\perp} . Clinical and pathologic studies have found that $\lambda_{//}$ tends to reflect axonal integrity, whereas λ_{\perp} corresponds more closely to myelin integrity (*DeBoy et al., 2007*). Animal and human studies suggest that $\lambda_{//}$ and λ_{\perp} are approximate measures of axonal and myelin integrity, particularly in acute injury (*Fox et al., 2010*).

Diffusion ellipsoids in highly organized fiber tracts (e.g., pyramidal tracts and the corpus callosum) are very elongated. The absence of fiber tracts in gray matter makes diffusion ellipsoids less elongated, though gray matter still demonstrates some anisotropy. FA is a common metric to describe the degree of diffusion directionality or elongation. A high FA within a single voxel would signify that diffusion occurs predominantly along a single axis. A low FA would signify that diffusion occurs along all 3 cardinal axes. An overall measure of diffusion magnitude is described by MD, which ignores anisotropy and simply describes the overall magnitude of diffusion (*Fox et al., 2010*).

Although routine structural MR images can accurately demonstrate brain tumors, they do not give precise information about the involvement and integrity of the white matter tracts in the immediate region surrounding tumors. Diffusion-tensor imaging may help in detection of white matter abnormalities in patients with malignant tumors in areas that appear normal on T2-weighted MR images, which raises the possibility that disruption of white matter tracts by tumor infiltration may be detectable by using diffusion-tensor imaging (*Provenzale et al., 2006*).

There are 2 main reasons why preoperative identification of white matter tracts is important. First, accurate localization of important white matter tracts can affect the decision of whether or not to operate. Secondly, preoperative localization of important white matter tracts is essential in surgical planning. (*Karimi et al., 2006*)

In this study, The hypothesis that diffusion tensor MR imaging can play a role in precise localization and assessment of the pertinent white matter tracts was assessed.

2. Material and Methods:

Study population:

32 patients (24 males and 8 females; age range 1-74 years; mean age 32.8±18 years) with intracranial neoplasms were included in this study. The tumors studied consisted of glioma (23 cases), metastasis (3 cases), lymphoma (one case), brain stem gliomas (3 cases) and meningiomas (2 cases).

MR Imaging Protocol:

A short acquisition time and instant processing are essential for the clinical feasibility of a certain procedure. We applied single-shot spin-echo echo-planar imaging (EPI) and parallel imaging techniques to achieve motion-free and higher signal-to-noise ratio (SNR) DTI. The total imaging time for DTI and FT was 7–9 minutes according to the section

numbers, which was added to the routine MR imaging examinations.

Acquisition of MR Images:

A 1.5-T MR unit (Gyrosan Intera; Philips Medical Systems, Best, the Netherlands) was used. The following sequences were acquired: T2-weighted sequences, fluid attenuated inversion recovery (FLAIR), T1-weighted sequences before and after intravenous administration of paramagnetic contrast material. DT imaging data were acquired by using a single-shot echo-planar imaging sequence with the sensitivity-encoding, or SENSE, parallel-imaging scheme (reduction factor, 2). The imaging matrix was 128 x 128, with a field of view of 220 x 220 mm. Transverse sections of 2.75mm thickness were acquired parallel to the anterior commissure–posterior commissure line. A total of 50 sections covered the entire hemisphere and brainstem without gaps. Diffusion weighting was encoded along 12 independent orientations, and the b value was 1000 mm²/sec. Other imaging parameters were as follows: echo time = 70 msec, repetition time = 6,599–8,280 msec, number of acquisitions = two. Coregistered magnetization-prepared rapid gradient-echo (MPRAGE) images of the same resolution were recorded for anatomic guidance.

H1 MR Spectroscopy was added in 25 cases, to characterize the nature of the tumor replacing biopsy.

The study was combined with fMRI in 15 cases to assess the relation of the tumor to the eloquent cortical areas, and use these areas as seed points in fiber tracking to precisely delineate the course of the pyramidal tract and separating the hands from the feet fibers.

Data processing:

We transferred the diffusion-tensor imaging data to an offline workstation (extended work space "EWS") (Release 2.5.3.0; Dell, Round Rock, Tex); Pride software (Philips Medical Systems) which is based on the Fiber Assignment by Continuous Tracking (FACT) method. Anisotropy was calculated by using orientation-independent fractional anisotropy (FA), and diffusion-tensor MR imaging–based color maps were created from the FA values and the three vector elements. The vector maps were assigned to red (x element, left-right), green (y, anterior-posterior), and blue (z, superior-inferior) with a proportional intensity scale according to the FA. Three-dimensional FT was then achieved by connecting voxel to voxel with the FACT algorithm. The threshold values for the termination of the fiber tracking were less than 0.3 for FA and greater than 45° for the trajectory angles between the ellipsoids.

Three-dimensional Tract Reconstruction:

To reconstruct tracts of interest, we used a multiple-region-of-interest (ROI) approach, which exploits existing anatomic knowledge of tract trajectories. Tracking was performed from all pixels inside the brain ("brute force" approach), and results

that penetrated the manually defined ROIs were assigned to the specific tracts associated with the ROIs. When multiple ROIs were used for a tract of interest, we used three types of operations, AND, OR, and NOT (Fig 1), the choice of which depended on the characteristic trajectory of each tract.

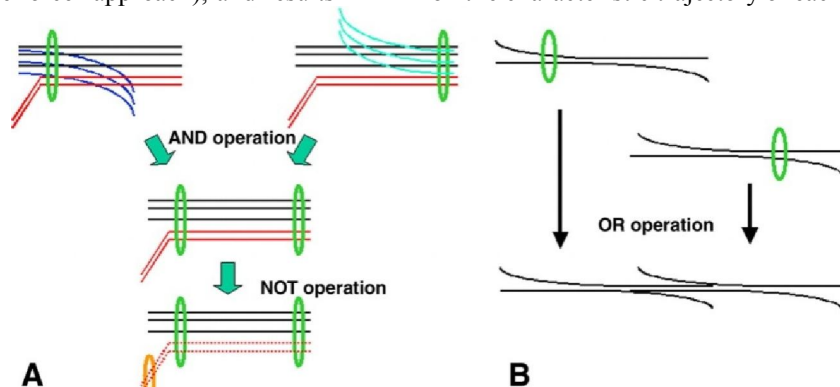


Figure 1. Diagram shows the three operations used in this study. *A*, AND and NOT operations. Two ROIs (green) are placed on anatomic landmarks. When the AND operation is used, tracts that penetrate both ROIs are selected. In this example, black and red tracts are selected, while blue tracts are removed. NOT operation is used to remove specific tracts that penetrate one or multiple ROIs (orange). In this example, red tracts are removed. *B*, OR operation. Multiple tracking results when multiple ROIs are combined. AND operation poses a strong constraint in tracking results by selecting only tracts with known trajectories. This is a conservative approach for which results are potentially more accurate, with the disadvantage that it does not allow visualization of branching patterns between ROIs. The OR approach may be more susceptible to noise and partial volume effects (*Quoted from Wakana et al., 2004*).

Tract evaluation with the aid of DT imaging:

Color-coded DTI maps were analyzed, followed by tractography of individual tracts. In most of patients the tumor was isolated to one hemisphere, and comparison was made between affected tracts by the tumor and the homologous tracts in the contralateral control hemisphere. White matter tracts were then characterized as: displaced (deviated), edematous, infiltrated and disrupted (destruction).

Displaced: if the tract showed normal or only slightly decreased FA, with abnormal location and/or direction, resulting from bulk mass displacement.

Edematous: if the tract maintained normal or slightly reduced anisotropy with normal orientation but demonstrated high signal intensity on T2WI.

Infiltrated: if the tract showed reduced anisotropy but remained identifiable on color maps.

Disrupted: if the tract showed isotropic (or near-isotropic) diffusion, such that it could not be identified on directional color maps.

Anatomic Landmarks and ROI Locations for Major White Matter Fibers:

For tracking of the white matter fibers, the region of interest (ROI) method was applied. We placed the single or multiple ROIs on the color maps. The plane of the ROI was varied according to the running direction of the white matter fibers (eg, corticospinal tract on the axial views, corpus callosum on the sagittal views).

For *corticospinal tract* tractography (*Fig. 2*), three ROIs were placed on transverse colour coded DT images according to established anatomic landmarks: The first ROI was placed in the pons anteriorly (where the CST is coded in blue), the second ROI was placed in the posterior limb of internal capsule, and the third ROI was placed at the motor cortex (precentral gyrus) which was identified on the basis of morphologic features of the sulci at the vertex. Fibers connecting the right and left corticospinal tracts via transverse pontine connection and fibers projecting into cerebellar peduncles were then removed by using the "NOT" operation because of apparent lack of compliance with classic definitions of the corticospinal tract.

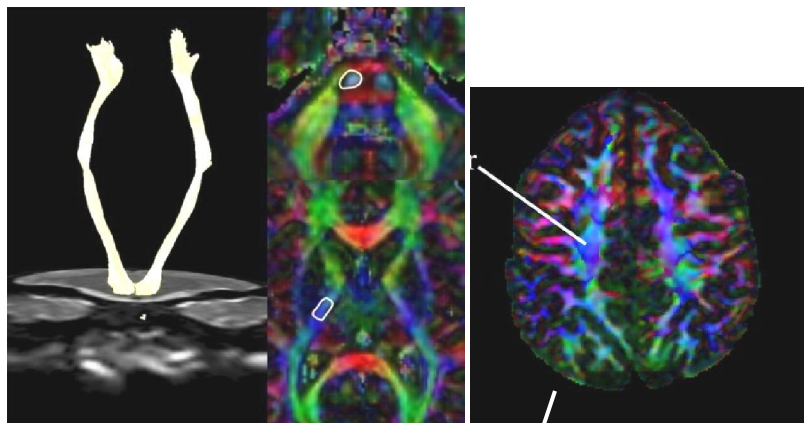


Fig 2: ROIS placement in CST fiber tracking

For the sensory tract, a pair of ROIs was placed at the dorsal part of the midbrain, pons, or both and the sensory cortex.

The superior longitudinal fasciculus was reconstructed at tractography by placing two ROIs in the cerebral deep white matter on a coronal directional color-coded map. The superior longitudinal fasciculus was identified on the coronal color-coded map as a region where the fiber orientation was anterior to posterior (green), lateral to the corona radiata (Mori *et al.*, 2002). An anterior ROI was placed in the plane passing through the reconstructed corticospinal tract, and a posterior ROI was placed in the plane passing through the rostral surface of the splenium of the corpus callosum, with both ROIs covering the green area representing the superior longitudinal fasciculus (Fig. 3). Some "noise" fibers that were apparently tracing the error course were then removed (Wakana *et al.*, 2004).

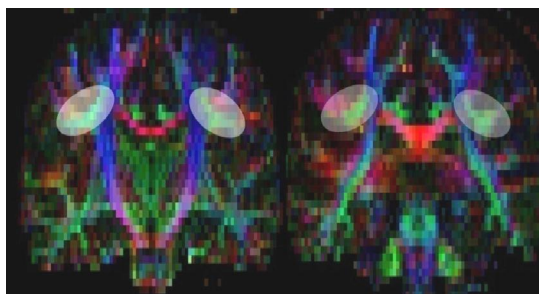


Fig 3: Coronal color-coded maps with ROIs (white ellipses). Anterior (left) and posterior (right) ROIs contain superior longitudinal fasciculus (green area lateral to corona radiata). (Quoted from Okada *et al.*, 2006)

Also, superior longitudinal fasciculus, one ROI was defined on a coronal section of the DT imaging-based color-coded maps at the posterior tip of the putamen. Fiber tracts of other longitudinal fibers like the *cingulum* (c) and *inferior longitudinal fasciculus* (ilf) are also generated from coronal images (Fig. 4).

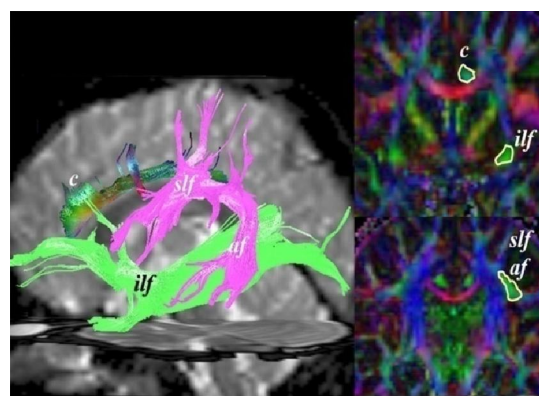


Fig 4: ROIs placement for tracking of association fibers. Cingulum (c), Superior longitudinal fasciculus (slf) Arcuate fasciculus (af), Inferior longitudinal fasciculus (ilf)

One ROI at the parieto-occipital sulcus, which was identified at the middle of the coronal section along the superior-inferior axis, was used for both the *inferior longitudinal fasciculus* and the *inferior fronto-occipital fasciculus*. For the inferior longitudinal fasciculus, an additional ROI was defined on a coronal section at the midtemporal lobe at the section level of the posterior tip of the putamen. For the inferior fronto-occipital fasciculus, an additional ROI was defined on a coronal section at the frontal lobe at the section level where the frontal and temporal lobes were separated. The ROIs for the inferior longitudinal fasciculus and the inferior fronto-occipital fasciculus were combined by using the operator AND.

Corpus callosum tractography was performed by imaging the combination of four different callosal fiber bundles. The primary ROI was placed in the corpus callosum in the midsagittal plane (Fig. 5). To visualize different parts of the callosal fibers, secondary ROIs were placed in four regions: two ROIs on the coronal color-coded map and two ROIs on the transverse color-coded map (Fig. 6). Anterior callosal fibers, referred to as minor forceps, were

reconstructed by placing the ROI covering the deep white matter in the coronal plane anterior to the genu of the corpus callosum. For reconstruction of the posterior callosal fibers, referred to as major forceps, the ROI was placed posterior to the splenium of the corpus callosum. Callosal body fibers were reconstructed by placing the ROI at the centrum semiovale in the transverse plane superior to the body of the corpus callosum. For reconstruction of the temporal interhemispheric connection fibers, referred to as tapetum, ROIs were placed bilaterally in the temporal deep white matter, lateral to the trigon of the lateral ventricles. These four fibers (ie, minor forceps, major forceps, callosal body fibers, and tapetum) were combined to delineate the entire corpus callosum (Okada et al., 2006).

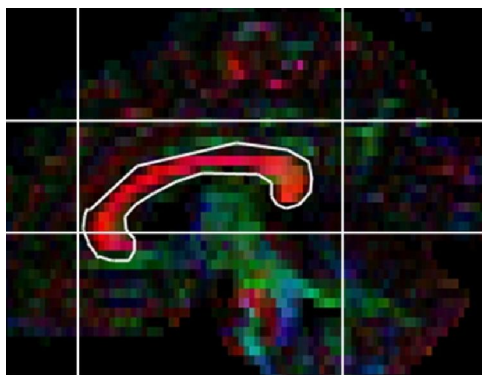


Fig 5: Primary ROI placed in corpus callosum on sagittal color-coded map. Vertical (coronal planes) and horizontal (transverse planes) white lines indicate section locations of secondary ROIs: anterior coronal section for minor forceps, posterior coronal for major forceps, superior transverse for body of corpus callosum, and inferior transverse for tapetum. (Quoted from Okada et al., 2006)

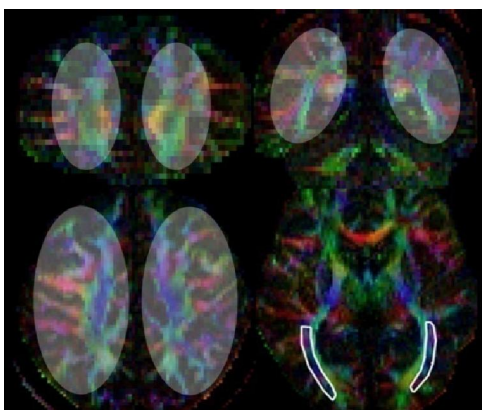


Fig 6: Transverse color-coded maps show secondary ROIs for corpus callosum: anterior ROIs for minor forceps (top left), posterior ROIs for major forceps (top right), superior ROIs for body of corpus callosum (bottom left), and inferior ROIs (white outlines) for tapetum (bottom right). (Quoted from Okada et al., 2006)

Limbic fibers through the fornix were reconstructed by placing one primary ROI and two secondary ROIs. The primary ROI was placed in the body of the fornix, and the secondary ROIs were placed in the crura of the right and left fornices anterolateral to the splenium of the corpus callosum (Fig. 7). (Okada et al., 2006)

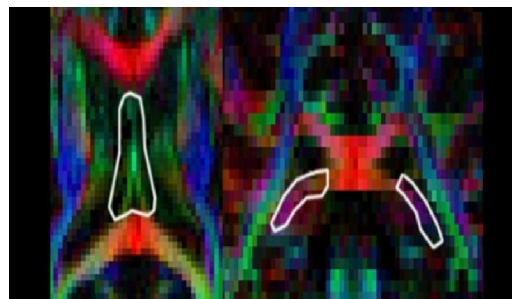


Fig 7: Transverse (left) and coronal (right) color-coded maps show ROIs (white outlines) for fornix. Primary (superior) ROI was placed at body of fornix (left); secondary (posterior) ROIs, at crura of fornices bilaterally (right). (Quoted from Okada et al., 2006)

Fiber tracking of the middle cerebellar peduncles was generated from single ROIs on the coronal view. These fiber tracts form a midline crossing by means of the transverse pontine fibers, and some extend to cortical connections superiorly (Fig. 8).

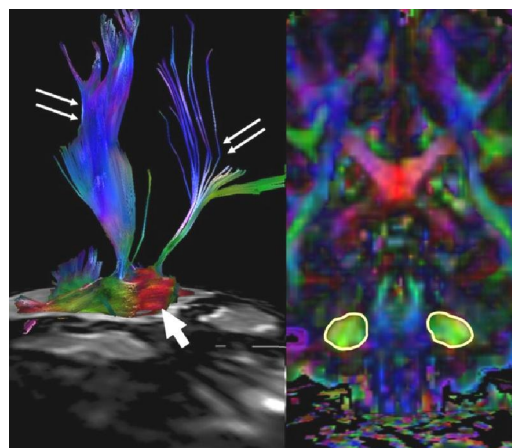


Fig 8: fiber tracking image of the middle cerebellar peduncles (left). Transverse pontine fibers (thick arrow), Cortical connections (thin arrows). ROIs placement on coronal colour map (right)

Fiber tracking of the *superior and inferior cerebellar peduncles* were generated from single ROIs on axial color maps (Fig. 9).

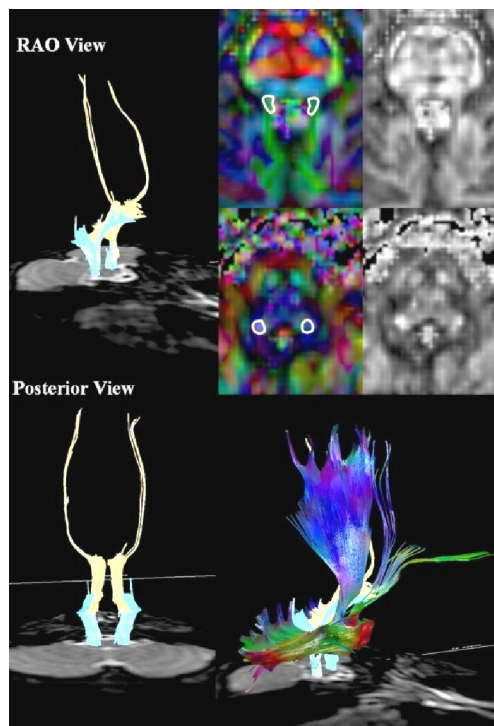


Fig. 9: Fiber tracking images of the superior (yellow) and inferior (blue) cerebellar peduncles (left and bottom right). ROIs on axial color maps (top right). RAO = right anterior oblique.

To reconstruct *optic radiation* tractography, the first "OR" ROI was placed on either side of the occipital lobe, including the calcarine cortex on coronal color-coded maps. The second "AND" ROI was at the ipsilateral temporal stem on sagittal color-coded mapping, including the Meyer loop. Most fibers in the temporal stem were green in the color-coded map, but the Meyer loop was red according to fiber direction and was distinguishable from other bundles. Various kinds of anteroposterior long association fibers or temporal projection fibers with diverting connectivity were included after these 2 ROI operations, such as the inferior occipitofrontal fasciculus and inferior longitudinal fasciculus. Based on the correlation between temporal fiber dissection and MR imaging, 2 more "NOT" ROI operations were applied to the ipsilateral temporal stem on coronal color-coded maps. One was lateral and the other medial to the Meyer loop. As a result, optic radiation tractography along the sagittal stratum was delineated (Fig. 10).

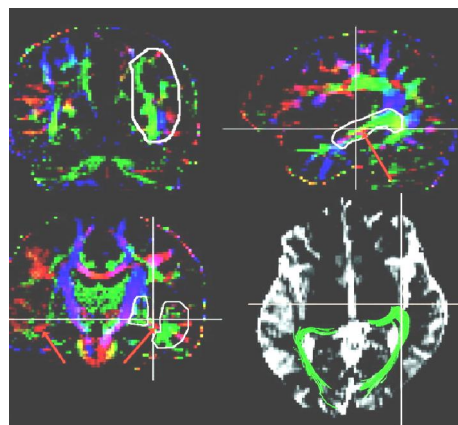


Fig 10: ROI segmentation for optic radiation tractography. The 4 kinds of ROIs (white polygon) are placed on coronal or sagittal color-coded maps. Cross lines indicate the orthogonal planes. The first "OR" ROI is placed at either side of the occipital lobe, including the calcarine cortex on the coronal plane through the anterior edge of the occipital-parietal sulcus (top left). The second "AND" ROI is placed at the ipsilateral temporal stem, including the Meyer loop on the sagittal plane (top right). Temporal stem is identified as green, and the Meyer loop is identified as a small red area inside the temporal stem (red arrow). The third and fourth "NOT" ROIs are placed on the same coronal plane through the dorsal end of the Sylvian fissure (bottom left). Bilateral Meyer loops are indicated as red arrows. Examples of bilateral optic radiation overlaid on transverse $b = 0$ images (TR/TE, 7000 ms/79 ms) are shown (bottom).

Presurgical tractographies of the *Meyer loop* (green in Fig. 11) were obtained with the seed area in the white matter that was located anterior to the lateral geniculate body and with the target area located in the ipsilateral sagittal stratum on the coronal planes at the level of the trigone.

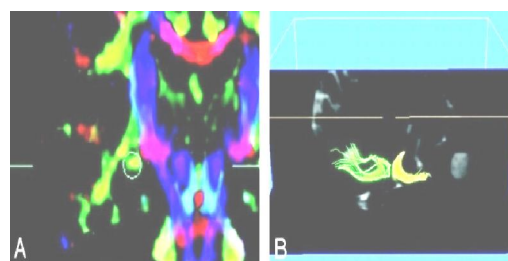


Fig 11: A, Coronal color coded map, the circle shows the seed area for the presurgical tractography. B, Tractography of the optic radiation (green) and uncinete fascicles is shown. Note that the 2 tracts are close together at the temporal stem. Thus, tractography of uncinete fascicles drawn in advance can be used as an assistant or a guide to draw the Meyer loop.

To help recognize the most anterior point of the Meyer loop in the presurgical images, we obtained tractographies of the *uncinate fasciculus* (yellow in

Fig. 11), which is located just anterior to the most anterior point of the Meyer loop. The seed area in the white matter of the frontal lobe was located on the coronal planes at the tip of the frontal horn of the lateral ventricle, and the target area in white matter was located on the coronal planes at the tip of the inferior horn of the lateral ventricle in the ipsilateral temporal tip.

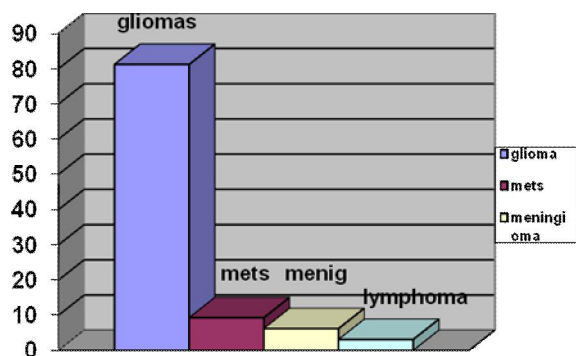
For reconstruction of the thalamic fibers, the entire thalamus was defined as the first ROI. The second ROI for the anterior and posterior thalamic radiations was placed on coronal sections to define the frontal lobe at the section level where the frontal and temporal lobes were separated and to define the occipital lobe at the section level of the posterior tip of the putamen, respectively. For superior thalamic radiation, the second ROI was defined on a transverse section above the corpus callosum, and it occupied the entire hemisphere. Again, the first and the second ROIs were combined by using the operator AND.

3. Results:

The population enrolled in this study comprises of 32 patients, 22(68.8%) were males and 10(31.3%) were females. Their age ranged from 1 to 74 years old with a mean age of 32.8 ± 18 .

The majority of the studied cases were above 40 years, and mostly males (68.8%), while females represents 31.3%.

The tumors studied consisted of 3 low grade gliomas, 10 grade II-III glioma, 2 grade III glioma, 5 glioblastoma multiforme, 3 gliomatosis cerebri, 3 metastasis, 1 lymphoma, 3 brain stem gliomas, 2 meningiomas (Graph 1)



Graph 1: Distribution of the studied cases as regard diagnosis

The diagnosis was based on biopsy and histopathology in 7 cases (21.8%), on H1 MR spectroscopy in 25 cases (78.2%).

Patients were classified into two main groups according to the tumor type:

1. Benign (including low grade gliomas, gliomatosis cerebri and meningiomas).
2. Malignant (high grade gliomas, metastasis and lymphoma).

Table (1) Comparison between both groups as regard general data

Variables	Benign N=11	Malignant N=21	X ²	P
Age				
≤10yrs	2(18.2%)	2(9.5%)		
11-20	1(9.1%)	4(19%)		
21-30	3(27.3%)	2(9.5%)	2.8	>0.05
31-40	2(18.2%)	4(19%)		NS
≥40	3(27.3%)	9(42.9%)		
Gender				
Male	5(45.5%)	17(81%)	4.2	<0.05
Female	6(54.5%)	4(19%)		S

This table shows that most of malignant group were males, while majority of benign group were females with significant difference in between by using chi-square test. No significant difference as regard age.

White matter pathway involvement was clearly identified in all patients by using color-coded DT imaging maps and 3D MR Tractography. Normal white matter pathways demonstrated on DT imaging appeared in the unaffected contra lateral hemisphere in 21 cases. Cases with bilateral tract involvement were compared with age matched normal controls.

The white matter tracts were color coded in a universal fashion based on their spatial orientation. Projection fibers were presented by blue color scheme, the commissural fibers were demonstrated by red color, and the association fibers were coded in green.

The white matter findings were characterized for each patient. White matter involvement by a tumor was classified according to the criteria of displacement, infiltration, disruption or edema. Displaced tracts maintained normal anisotropy but were situated in abnormal location or with abnormal orientation on color coded maps; edematous tracts maintained normal anisotropy and orientation but demonstrated high signal intensity on T2WI on conventional MRI. Infiltrated tracts showed reduced anisotropy but remained identifiable on orientation maps; and disrupted tracts showed markedly reduced anisotropy such that could not be identified on orientation maps. The involvement of the anatomically assigned pathways in the two main groups is summarized in the following tables:

Table (2) Comparison between both groups as regard MRI findings (edema)

Edema	Benign N=11	Malignant N=21	X ²	P
No	9 (81.8%)	16 (76.2%)	0.13	>0.05 NS
Yes	2 (18.2%)	5 (23.8%)		

This table shows that prevalence of edema was higher among malignant group in comparison to benign group but with no significant difference in between by using chi-square test.

Table (3) Comparison between both groups as regard MRI findings (displacement)

Displacement	Benign N=11	Malignant N=21	X ²	P
No	1 (9.1%)	9 (42.9%)	3.8	<0.05 S
Yes	10(90.9%)	12 (57.1%)		

This table shows that prevalence of displacement was higher among benign group in comparison to malignant group with significant difference in between by using chi-square test.

Table(4) Comparison between both groups as regard MRI findings (infiltration)

Infiltration	Benign N=11	Malignant N=21	X ²	P
No	6 (54.5%)	9 (42.9%)	0.4	>0.05 NS
Yes	5 (45.5%)	12 (57.1%)		

This table shows that prevalence of infiltration was higher among malignant group in comparison to benign group but with no significant difference in between by using chi-square test.

Table (5) Comparison between both groups as regard MRI findings (disruption)

Disruption	Benign N=11	Malignant N=21	X ²	P
No	10(90.9%)	9 (42.9%)	4.5	<0.05 S
Yes	1 (9.1%)	12 (57.1%)		

This table shows that prevalence of disruption was higher among malignant group in comparison to benign group with significant difference in between by using chi-square test.

Analysis of data was done by IBM computer using SPSS (statistical program for social science version 12) as follows :

Description of quantitative variables as mean, SD and range

Description of qualitative variables as number and percentage

Chi-square test was used to compare qualitative variables between groups.

P value >0.05 insignificant P<0.05 significant

P<0.01 highly significant

4. Discussion

Neurosurgery for a brain tumor is a trade-off between maximum surgical resection on one hand and maximum sparing of functions on the other hand. Extensive tumor resection can reduce the risk of relapse (particularly gliomas with low grade malignancy) and allow subsequent radiotherapy or chemotherapy to be more effective. On the other hand, sparing "functionally relevant" zones and therefore preservation of motor, visual or language functions significantly improves the quality of life of these patients (*Romano et al., 2007*). For realizing these goals, many imaging modalities were used to assess brain tumors, which include conventional MRI, Positron Emission Tomography and functional MRI (*Fujiwara et al., 2004*). Knowledge of the structural integrity and location of certain white matter tracts with respect to an intracranial lesion is crucial for neurosurgical planning, both for defining the surgical access point and identifying the extent of tumor resection (*Romano et al., 2007*).

DTI is a significant advancement in the field of diagnostic imaging. It is, in fact, the only method capable of displaying cerebral white matter tracts in vivo, and it has been shown that this knowledge can assist the neurosurgeon in preoperative planning (*Yu et al., 2005*).

Diffusion- tensor imaging provides information on the directionality of water molecules at the cellular level, thus indicating the orientation of fiber tracts. From DW image data sets, the diffusivity of water within tissue can be determined. In tissue with an ordered microstructure, like cerebral white matter, orientation can be quantified by measuring its anisotropic diffusion. Diffusion- tensor calculations permit the characterization of diffusion in heterogeneously oriented tissue. The spatial orientation of myelinated fiber tracts can then be represented as distinct white matter maps in easily read, color-coded directional maps (*Witwer et al., 2002*). Recently, various investigators have used directional diffusion information to create maps of white matter connectivity (*Stieltjes et al., 2001*). These techniques may be valuable for tract identification when the white matter tracts are displaced by tumor (*Witwer et al., 2002*).

The most significant use of DTI, in particular, is to preoperatively confirm the integrity and location of displaced white matter tracts (*Romano et al., 2007*).

White matter tracts may be pathologically altered by tumor in several ways; specifically, they may be displaced, infiltrated by tumor and/or edema, or destroyed. Four imaging patterns were identified that presumably reflected these alterations on FA-weighted directional color maps. Unfortunately,

however, these alterations are not mutually exclusive in a given tumor or even in a given white matter tract. (Field *et al.*, 2004).

Our study, being the first to be conducted in our department of radiology, in Ain Shams University, aimed at exploring the value of the state of the art Diffusion Tensor MR Imaging in the preoperative assessment of brain tumors. The study was conducted on 32 patients with different types of brain tumors, to demonstrate how DT mapping further elucidate the complex relationship between a lesion and its surrounding white matter. Their age ranged from 1 to 74 years old with a mean age of 32.8 ± 18 years.

The majority of the studied cases were above 40 years, and mostly males (68.8%). The most frequent neurological clinical presentation was hemiparesis.

The tumors studied consisted of 3 low grade gliomas, 10 grade II-III glioma, 2 grade III glioma, 5 glioblastoma multiforme, 3 gliomatosis cerebri, 3 metastasis, 1 lymphoma, 3 brain stem gliomas, and 2 meningiomas.

Conventional contrast enhanced MRI followed by MR Diffusion Tensor Imaging were acquired in all of the studied population. H1 MR Spectroscopy was added in 22 cases, and combined fMRI- DTI was performed in 15 cases.

White matter tracts involvement by a tumor was categorized into four patterns on DT mapping and Tractography, these are: *edema*, *displacement*, *infiltration* and *disruption*. Quantitative analysis was also obtained by measuring the FA and ADC values of each affected tract, with comparison with the contra lateral homologous tracts in the unaffected hemisphere in unilateral tumors, or age and sex matched controls in bi-hemispheric or brain stem lesions.

This classification of tract involvement was similar to the studies done by Witwer *et al.*, 2002 and Field *et al.*, 2004. However, this was slightly different from the classification done by Yu *et al.*, 2005, who divide the relationship between tumor and tracts into three types only; type I: simple displacement, type II: displacement with disruption, type III: simple disruption.

In the present study we classified the patients into two groups: *Benign group*: including low grade and benign tumors, and, *malignant group*: including high grade glial tumors, metastasis and lymphoma.

There was a statistical difference between these groups, with prevalence of displacement among benign group and disruption among the malignant group with P value < 0.05 . This in contrary to the effect of edema and infiltration where there was no significant difference between the two groups, with P value > 0.05 . This partially agreed with the study done by Field *et al.*, 2004. They identified

displacement and edema patterns in both benign and malignant tumors. Infiltration was limited to infiltrating gliomas, but there were only two of these. Destruction was limited to malignant tumors, in both high and low grade malignancies. This signifies that DTI has a potential role in characterization of brain tumors and differentiation between benign and malignant neoplastic lesions.

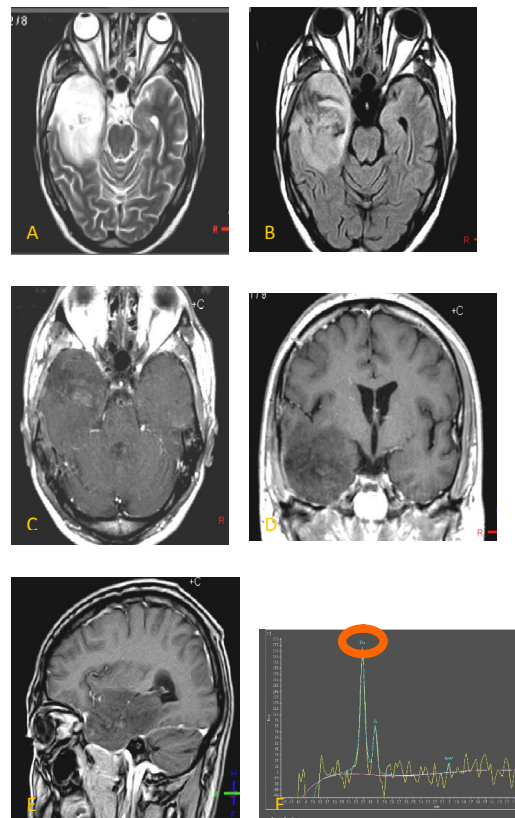


Fig. 12: 36 years old male patient known to have right temporal glioma and coming for follow up after therapy.

A) Axial T2WI MR image: Right temporo-parietal infiltrative expansive hyper intense SOL .

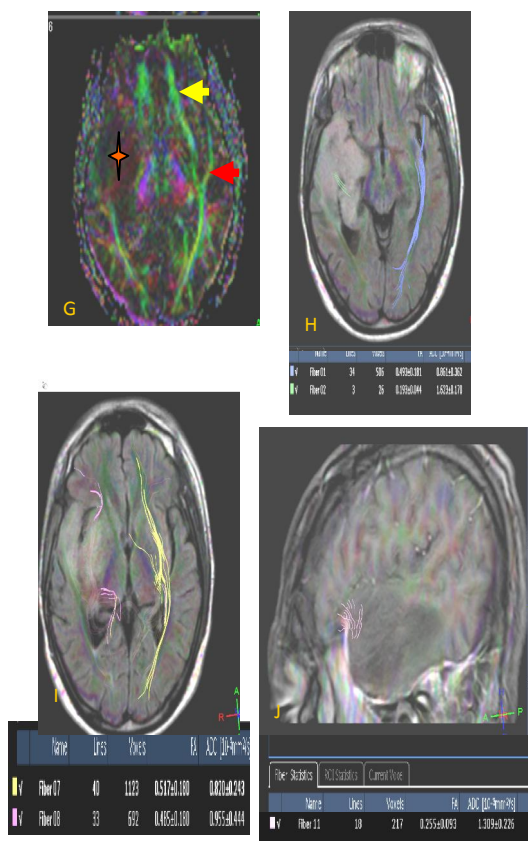
B) Axial FLAIR MR image "at the same level of A": the lesion exhibits heterogeneous, predominantly high, signal with minimal surrounding edema .

C) Axial post contrast T1WI +MTC: there is a small enhancing portion at infero-medial aspect of the lesion and inner non enhancing necrotic areas.

D) , E) Coronal (D) and sagittal (E) contrast enhanced T1WI : the lesion is faintly enhancing.

F) H1-MR Spectroscopy (single voxel, intermediate echo spectrum; TE=144): the lesion shows evident elevation of choline , denoting accentuated cell membrane turnover, especially at the enhancing portion.

MR Perfusion (not shown) revealed remarkable elevation of perfusion with rCBV ratio reaching 4 as compared to contra lateral normal side.



g) Axial color coded DTI map: the intact green fibers of the inferior longitudinal fasciculus (ILF) (red arrow) and the inferior occipito frontal fasciculus (IOF) (yellow arrow) within the unaffected temporal lobe of the left hemisphere are well identified. Corresponding fibers in the contra lateral temporal lobe are completely obliterated within the lesion (red asterix).

H) Tractography of both ILF: axial color coded DTI map overlaid on axial FLAIR MR image demonstrating intact fibers in the left side with normal course, while on the right side the fibers are disrupted with marked reduction of the FA values of the remaining identifiable fibers compared to the normal side with reciprocal increase in the ADC value.

I) Tractography of both IOF: axial color coded DTI map overlaid on axial FLAIR MR image demonstrating intact fibers in the left side, while on the right side the fibers are barely identified with marked reduction of the FA values of the remaining identifiable fibers compared to the normal side with reciprocal increase in the ADC value.

j) Tractography of the right uncinus fasciculus: sagittal color coded DTI map overlaid on sagittal post contrast T1WI MR image: the fibers appears disrupted with marked loss of anisotropy and increase in diffusivity.

The DTI and Tractography findings are in keeping with the diagnosis of high grade neoplasm as evident by disruption of the related fiber tracts.

We recommend to do gross total resection without undue concern for preserving these tracts or risking new functional deficits postoperatively.

Several studies have addressed the problem of discrimination between bland edema (tumor free) from infiltrating tumor (tumorous edema) through the analysis of ADC and FA values with mixed results. *Tropine et al., 2004*, demonstrated that DTI may not

reliably distinguish tumor infiltration from vasogenic edema in supratentorial gliomas glioblastomas. *Price et al., 2003* examined peritumoral DTI white matter "signatures" at 3 T field strength and concluded that more work is needed to establish the relationship between DTI parameters and tumor characteristics. *Sinha et al., 2002*, found significant difference of ADC values among apparently normal white matter, edematous brain and enhancing tumor margins, with the diffusion anisotropy data added no benefit in tissue differentiation. *Lu et al., 2003*, demonstrated that there are clear differences in the diffusion characteristics of the vasogenic edema surrounding brain tumors, when compared with those of normal-appearing white matter. In addition, peritumoral MD specifically may be useful in the preoperative discrimination of high-grade gliomas and metastatic tumors; however, the changes in FA showed no such statistical significance. The comparable decrease in FA for both disease processes is attributable to a large water influx surrounding metastatic tumors and contributions of both increased water content and tumor infiltration surrounding gliomas.

The present study must be encountered among those that were unable to discriminate tumor from edema on the basis of ADC and FA values alone. However, we have taken an additional step by analyzing the directional color map and performing tractography for the affected fibers, and our preliminary results are encouraging. We found that vasogenic edema in the absence of bulk mass displacement tends to exhibit reduced FA without associated directional changes, as reflected by normal hues on directional color maps. This is in contrast to infiltrating tumors, where the FA reduction was accompanied by a more severe form of disorganization reflected in abnormal hues on directional color maps. There did not appear to be sufficient bulk mass displacement to account for these changes. These findings strongly agreed with *Field et al., 2004*.

One situation in which DTI has high diagnostic capability is in cases of gliomatosis cerebri, which has a specific histopathological behavior. The neoplastic cells form parallel rows among nerve fibers preserving them, yet with destruction of the myelin sheath (*Cruz and Sorensen, 2006*). This results in preservation of the location and orientation of the fiber tracts on color coded DTI mapping with mild reduction of FA values of the involved tracts.

Three cases of gliomatosis cerebri were included in this current study, one of them was proved by histopathology, and two cases were diagnosed based on MR spectroscopy and MR perfusion data (*Fig. 13*). The DTI functional anisotropy maps and Tractography demonstrated that

the related fiber tracts were preserved, yet with mild reduction of in their FA values, reflecting normal underlying cytoarchitectural pattern of the nerve fibers.

As regard the brain stem tumors *Heltona et al., 2006*, had the first study to evaluate the quantitative the quantitative DTI measures of FA and ADC in pediatric patients with diffuse and focal **pontine tumors** and in those with "normal" brain stem, as determined by conventional MR imaging. Their results indicated that DTI analysis can delineate tract invasion and displacement. These tools may help to better discriminate between diffuse and focal brain stem **tumors** in the future and may be useful for guiding surgical biopsies. DTI analysis also shows promise of providing quantitative measures of risk stratification, prognosis, and treatment response.

This study included 3 cases with infiltrative pontine gliomas, two of them was in the pediatric age group. DTI has well demonstrated the affection of brain stem fiber tracts including; the corticospinal tract, medial lemniscus and transverse pontine fibers with various degrees of involvement as deduced from the quantitative ADC and FA measures as well as fiber tracking. The conventional MRI features was typical for infiltrative gliomas in the pediatric cases, however, it was slightly deceiving in the adult case. The lesion exhibited focal enhancement pattern while DTI demonstrated infiltration of the tracts beyond the enhancing tumor margin evident on DT color map and Tractography. This was confirmed by MR spectroscopy, showing evident elevation of Choline metabolic peak beyond the enhancing margin denoting neoplastic infiltration.

Diffuse pontine tumors comprise a group of malignant tumors with a much poorer prognosis than that of focal brain stem tumors. Pontine tumors account for about 15% of pediatric brain tumors and comprise approximately 20%–30% of posterior fossa tumors. Histopathologically, these diffuse pontine tumors are usually differentiated WHO grade II fibrillary astrocytomas or WHO grade III anaplastic astrocytomas at diagnosis and are known to infiltrate between normal axonal fibers (*Lesniak et al., 2003*). Although the appearance of focal brain stem tumors and that of diffuse brain stem tumors typically differ by conventional MR imaging, distinguishing focal from diffuse involvement is sometimes imprecise. The discovery of a method that distinguishes these 2 types of tumors is valuable because the treatment and prognosis for the brain stem tumors are substantially different. On T2-weighted MR images, focal tumors are typically well marginated, often enhance, may be exophytic, and occupy <50% of the axial diameter of the brain stem, whereas diffuse tumors are poorly marginated, rarely enhance, occupy more than 50%

of the axial diameter of the brain stem, lack an exophytic component, and commonly engulf the basilar artery (*Barkovich, 2000*).

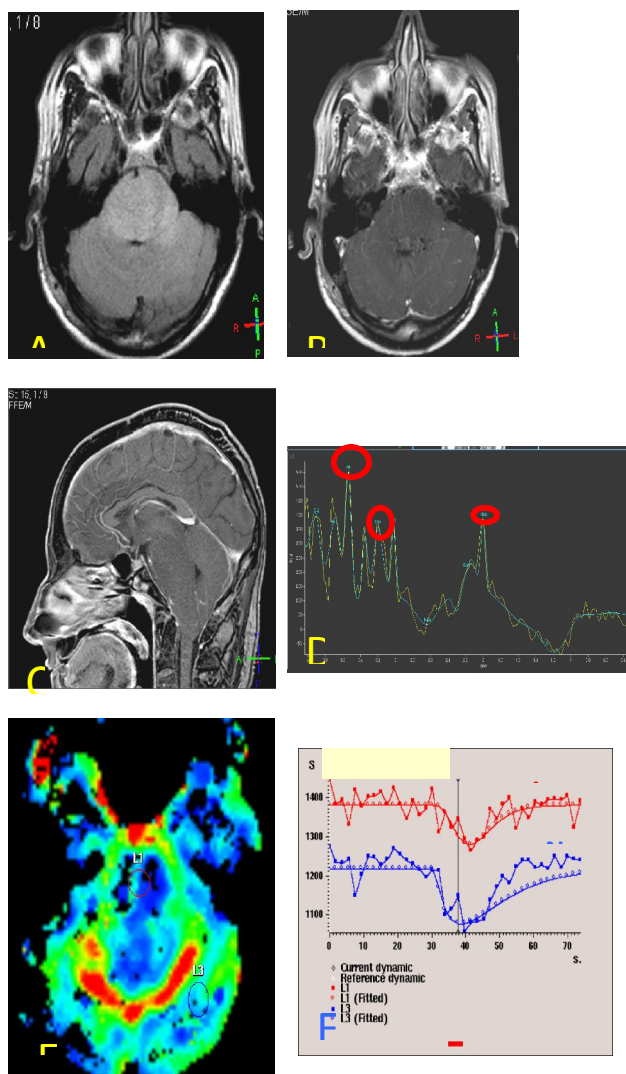
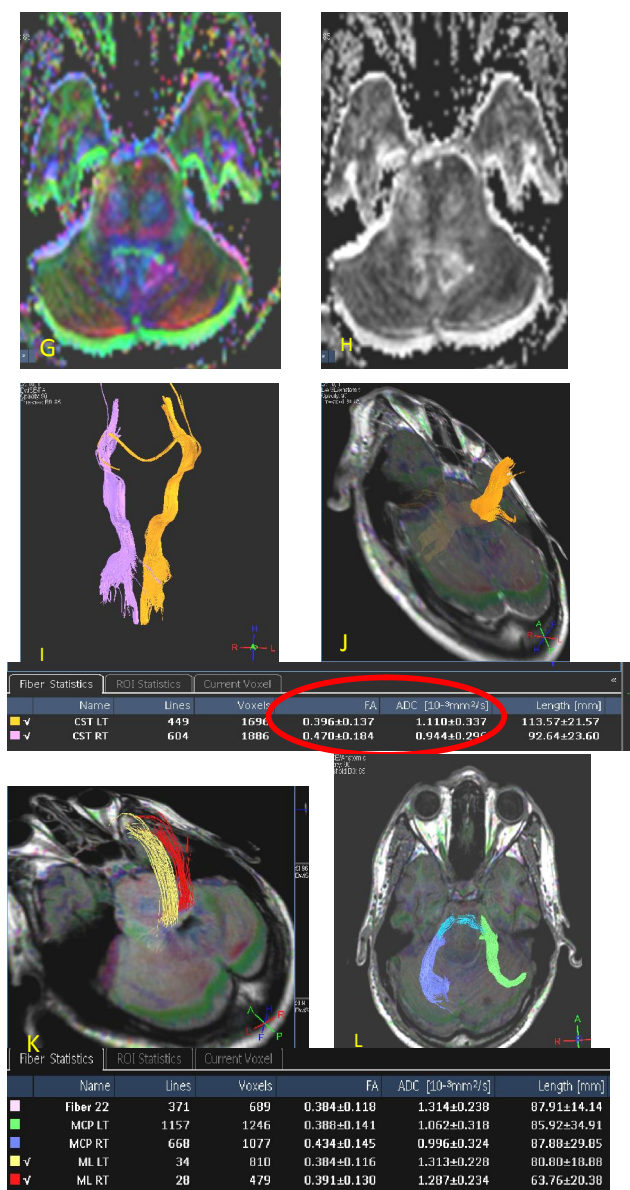


Fig. 13: 47 years old male patient complaining of symptoms of raised intracranial tension. He underwent ventriculo-peritoneal shunt to relieve his symptoms.

- A. Axial FLAIR MRI** shows diffuse signal abnormality and enlargement of the Pons with involvement of the cerebellum through the middle cerebellar peduncles. The fourth ventricle is encroached upon and attenuated.
- B. Axial post contrast T1WI+MTC:** The lesion does not show any enhancement.
- C. Sagittal post contrast T1WI :** The lesion extends to involve the medulla and midbrain with relative preservation of underlying brain architecture.
- D. H1 MR Spectroscopy,** single voxel, intermediate echo spectra (TE=144) shows marked elevation of myoinositol (mI), mildly increased choline (Cho) and decreased NAA.
- E. MR Perfusion color coded map:** the lesion is hypovascular.
- F. MR Perfusion dynamic curves** show low rCBV of the lesion (value of 1) compared to normal cerebellar hemisphere (value of 2.8) which correlates with lack of vascular hyperplasia.



G. Axial color map at the level of the brain stem: The corticospinal tracts coded in blue are expanded yet retaining their anatomical site and orientation with normal color hue (red arrow). The transverse pontine fibers (green arrow) and medial lemniscus (black arrow) are also involved but to a lesser extent. The ML fibers are backwardly displaced by virtue of the expanded CST.

H. Axial FA map at the same level: the brain stem tracts show mildly reduced anisotropy.

I. Tractography of the both CST: The fibers are retaining their normal location with maintained FA values.

J. Tractography of the left CST overlaid on anatomical T1WI+color coded map: the tracts are passing unaffected through the tumor denoting normal underlying cytoarchitectural pattern. , L)

K. Tractography of both ML (K) and MCP (L) overlaid on axial 3D T1WI+color coded DT map. The tracts same findings as in Fig. J.

Conventional MR imaging has demonstrated prognostic value in the treatment of brain stem tumors, but white matter appears homogeneous on MR images; therefore, this method cannot precisely define essential aspects of tract location, displacement, or invasion. In contrast, diffusion tensor imaging (DTI) detects anisotropic diffusion, thereby allowing the visualization of major fiber tracts in the brain stem. Thus, DTI may provide information about tumor involvement in white matter tracts (*Helton et al., 2006*).

As a part of self criticism, our study was lacking the postoperative follow up the patients to validate the impact of DTI on surgical planning ,as all the cases were performed in an out patient radiology center and not in hospital institution.

The preoperative depiction of a tumor relationships to white matter tracts using DTI and directional color mapping proved to be extremely useful to the neurosurgeons in a study done by *Field et al., 2004*. knowing that a white matter tract was intact but displaced by a tumor to a new location allowed the surgeon to adapt his approach to preserve this tract during resection. Similarly, knowing that a specific white matter tracts were destroyed by a tumor allowed the surgeon to attempt gross total resection without undue concern for preserving these tracts of risking new functional deficits postoperatively. Neurosurgeons at the authors' institution now obtain preoperative DTI routinely for any tumors thought to potentially involve critical white matter fiber tracts.

Yu et al., 2005, proposed to try one 's best to preserve displaced white matter tract while maximizing tumor resection, to enlarge the extent of tumor resection while preservation of the displaced part of the tract in cases where destruction and displacement of the tract co-exist, and maximize tumor resection while preservation of the residual part of the tract in cases with simple disruption.

Functional MRI was combined with DTI as a preoperative assessment for surgical planning of brain tumors in 15 cases in this study. We used the cortical activation areas as seed points to improve fiber tracking results. Also, we obtained essential information on the location of eloquent cortical areas in relation to a tumor to determine the risk of injury during surgery. The integration of both high-resolution anatomic (T1-weighted) data with fMRI data in the fiber-tracking procedure made an evaluation of the spatial relationship between tracked fibers and tumor borders possible. Separation of the different components of the corticospinal tract especially the hands and feet fibers was also possible.

Smits et al., 2007 had incorporated FMRI and DTI in the preoperative assessment in a series of

patients with brain tumors. They showed that tracking of the CST directly from the fMRI activation area can be used to visualize and distinguish the different components of the CST, especially the hand and foot fibers. In a healthy volunteer, the presented method showed that the tracked hand, foot, and lip fibers follow a distinct course, the foot fibers coursing posteromedially to the hand fibers within the posterior limb of the internal capsule (PLIC). This distribution within the corticospinal tract confirmed previous findings by *Holodny et al., (2005)* who also studied the CST by using DT tractography and found the same location and internal organization of the separate CST components within the PLIC. Both studies indicate that the hand and foot fibers are organized along the short (left-right) axis of the PLIC, rather than along the long (anteroposterior) axis of the PLIC, as has been previously assumed. (*Gray, 1989*)

Smits et al., showed that tracking the CST based only on anatomic landmarks may not be sufficient to visualize reliably the CST and that fMRI-based seed region-of-interest placement may be necessary to visualize the CST in its entirety. Furthermore, DT tractography of the CST was seen to be hampered in cases of anatomic distortion due to a mass effect of the lesion or in cases of altered diffusivity due to tumor infiltration or perifocal edema in the region of the CST. Tracking improved when the fMRI-based seed region-of-interest approach was used, thus providing more reliable preoperative information.

Several limitations need to be considered :

Firstly, there is no "gold standard" for in vivo Tractography. In fact, DTI is the only method that permits the calculation and visualization of fiber tracts trajectories in vivo.

Secondly, DTT is a user defined process. In particular, the tracking results were found to vary according to FA threshold, angular threshold, step length and numbers of sampling in a voxel length. Choosing different parameters can produce different fibers. And tracked volumes are also dependent on the size and locations of the seed ROIs.

Despite these intrinsic limitations, our study clearly showed that this technique can be very useful for correct preoperative planning and should be considered an important step forward in modern neuroradiological diagnostics for surgical planning in patients suffering from intracranial tumors.

In conclusion, the effect of cerebral neoplasm on white matter pathways is much more better evaluated with the aid of DTI than on conventional MRI. There can be one or more of four distinct patterns of white matter tracts alteration by a tumor. In this small cohort of patients the information provided by DT imaging further defined precise

relationships between the sub cortical white matter structures and the cerebral neoplasm. This potentially has a role in tumor characterization, and more importantly in surgical planning. MR Tractography offers the neurosurgeon an anatomical panoramic view and the opportunity for improved planning of surgical resection of intracranial lesions and in predicting the extent of safe resection.

Despite its limitations and potential pitfalls, DTI has proven to be the only clinically feasible method of demonstrating the white matter tracts *in vivo*.

Combination of fMRI and DTI fiber tracking appears to be a more promising tool in the preoperative planning of brain tumors. fMRI-based DT tractography is superior to DT tractography on the basis of anatomic landmarks alone, because only with fMRI-based DT tractography is a distinction between the several components of the CST possible. Furthermore, it allows decreasing the FA threshold if necessary and provides an improved visualization of the CST, in particular when fiber tracking is hampered by the presence of tumor or perifocal edema.

These new techniques should be considered an important step forward in modern neuro-radiological diagnostics for surgical planning of cerebral neoplasm.

Corresponding author

Mohsen Gomaa and Yosra abdel zaher
Department of Radiodiagnosis, Ain Shams University
mostafa_redio@yahoo.com

References:

1. Barkovich AJ. Pediatric neuroimaging. In: Barkovich AJ. Intracranial, Orbital, and Neck Tumors of Childhood. 3rd ed. Philadelphia, Pa: Lippincott Williams & Wilkins;2000 :462–70
2. Basser PJ, Pierpaoli C Microstructural and physiological features of tissues elucidated by quantitative-diffusion-tensor MRI. J Magn Reson 1996;111:209–19
3. Cruz CH and Sorenson AG. Diffusion Tensor Magnetic Resonance Imaging of Brain Tumors. Magn Reson Imaging N Am 2006;14:183-202
4. DeBoy CA, Zhang J, Dike S, et al High-resolution diffusion tensor imaging of axonal damage in focal inflammatory and demyelinating lesions in rat spinal cord. Brain 2007;130:2199–210
5. Fox R.J., Cronin T, Lin J., Wang X., Sakai K, Ontaneda D, Mahmoud SY, Lowe MJ, and Phillips MD. Measuring Myelin Repair and Axonal Loss with Diffusion Tensor Imaging AJNR Am J Neuroradiol 2011 32: 85-91.

6. Field AS, Alexander AL, Hasan KM, Wu YC, Witwe B and Badie B. Diffusion tensor eigenvector directional color imaging patterns in the evaluation of cerebral white matter tracts altered by tumor. *Journal of Magnetic Resonance Imaging* 2004;20:555-562.
7. Fujiwara N, Sakatani K and Katayama Y. Evoked-cerebral blood oxygenation changes in false negative activations in BOLD contrast functional MRI of patients with brain tumors. *Neuroimage* 2004;21:1464-71.
8. Gray H. *Neurology*. In: Williams P, Warwick R, Dyson M, et al., eds. *Gray's Anatomy*. Edinburgh, UK: Livingstone; 1989:1073
9. Heltona KJ, Phillipsa NS, Khana RB, Boopc FA, Sanfordc RA, Zoua P, Lib CS, Langstona JW and Ogga RJ. Diffusion Tensor Imaging of Tract Involvement in Children with Pontine Tumors *American Journal of Neuroradiology* 2006;27:786-793.
10. Holodny AI, Gor DM, Watts R, et al. Diffusion-tensor MR tractography of somatotopic organization of corticospinal tracts in the internal capsule: initial anatomic results in contradistinction to prior reports. *Radiology* 2005;234:649-53
11. Karimi S, Nicole M, Kyang K, et al. Advanced MR techniques in brain tumor imaging. *Appl.Rad.* 35(5):9-18,2006.
12. Lesniak MS, Klem JM, Weingart J, et al. Surgical outcome following resection of contrast-enhanced pediatric brainstem gliomas. *Pediatr Neurosurg* 2003;39:314-22
13. Lu S, Ahn D, Johnson G, Cha S. Peritumoral diffusion tensor imaging of high-grade gliomas and metastatic brain tumors. *AJNR Am J Neuroradiol* 2003;24:937-41.
14. M. Clinton Miller, Ph.D, Rebecca G. Knapp: *Clinical epidemiology and biostatistics*, published by Williams & Wilkins, Maryland: 3rd edition 1992.
15. Mori S, Frederiksen K, Van Zijl PCM, Stieltjes B, Kraut MA, Slaiyappan M, et al. Brain white matter anatomy of tumor patients evaluated with diffusion tensor imaging. *Ann Neurol* 2002;51: 377-80.
16. Pierpaoli C, Basser PJ. Toward a quantitative assessment of diffusion anisotropy. *Magn Reson Med* 1996;36:893-906
17. Okada T, Miki Y, Fushimi Y, et al. Diffusion-tensor fiber tractography: intraindividual comparison of 3.0-T and 1.5-T MR imaging. *Radiology* 2006;238:668-678.
18. Price SJ, Burnet NG, Donovan T, Green HAL, Pena A, Antoun NM, et al. Diffusion tensor imaging of brain tumors at 3T: a potential tool for assessing white matter tract invasion. *Clin Radiol* 2003;58:455-62.
19. Provenzale JM, Mukundan S and Barboriak DP. Diffusion weighted and perfusion MR imaging for brain tumor characterization and assessment of treatment response. *Radiology* 239:632-649.2006.
20. Romano A, Ferrante M, Cipriani V, Fasoli F, Andrea GD, Fantozzi LM, Bozzao A. Role of magnetic resonance tractography in the preoperative planning and intraoperative assessment of patients with intra-axial brain tumours. *Radiol med* 2007;112:906-920.
21. Sinha S, Bastin ME, Whittle IR, et al. Diffusion tensor MR imaging of high-grade cerebral gliomas. *AJNR Am J Neuroradiol* 2002;23:520-27
22. Smits M, Vernooij MW, Wielopolski PA, Vincent AJPE, Houston GC and van der Lugta A. Incorporating Functional MR Imaging into Diffusion Tensor Tractography in the Preoperative Assessment of the Corticospinal Tract in Patients with Brain Tumors. *American Journal of Neuroradiology* 2007; 28:1354-1361.
23. Tropine A, Vucurevic G, Delani P, et al. Contribution of diffusion tensor imaging to delineation of gliomas and glioblastomas. *J Magn Reson Imaging* 2004;20:905-12
24. Wakana S, Jiang H, Nagae-Poetscher LM, van Zijl PC, Mori S. Fiber tract-based atlas of human white matter anatomy. *Radiology* 2004; 230:77-87.
25. Witwer BP, Moftakhar R, Hasan KM, Deshmukh P, Haughton V, Field A, et al. Diffusion-tensor imaging of white matter tracts in patients with cerebral neoplasm. *J Neurosurg* 2002; 97:568-75.
26. Yu CS, Li KC, Xuan Y, Ji XM and Qin W. Diffusion tensor Tractography in patients with cerebral tumors: A helpful technique for neurosurgical planning and postoperative assessment. *European Journal of Radiology* 2005; 56: 197-204.